Bayesian Combined Analysis of JET LIDAR, Edge LIDAR and Interferometry Diagnostics.

O. P. Ford[1], J. Svensson[2], M. Beurskens[3], A. Boboc[3], J. Flanagan[3], M. Kempenaars[3], D. C. McDonald[3], A. Meakins[3] and JET EFDA contributors*

JET-EFDA, Culham Science Centre, OX14 3DB, Abingdon, UK

[1] *Blackett Laboratory, Imperial College, London SW7 2BZ, UK*

[2] *Max Planck Institute for Plasma Physics, Teilinstitut Greifswald, Germany*

[3] *Euratom/UKAEA Fusion Association, Culham Science Centre, Abingdon, OX14 3DB, UK*

Introduction

The accurate determination of electron density n_e and temperature T_e is important for many areas of Tokamak research. On JET, several diagnostics make observations which are usually analysed independently to infer n_e and T_e. Combining such results to obtain a single complete picture of T_e and n_e is complicated by the varying location, spatial resolution and physical processes of the diagnostics and by the assumptions and accuracies of the different analyses. Bayesian analysis and forward modelling are used in this paper to obtain a single consistent picture of what can be known about N_e and T_e from the observations of the Interferometry[1], core LIDAR[2] and edge LIDAR[3] diagnostics and a single set of prior assumptions.

The interferometry measures accurate line-integrated density along 8 line of sights in the poloidal plane. Two LIDAR systems measure the spectrum of Thomson back-scattered light, from a $\sim 300ps$ laser pulse. The core LIDAR laser passes approximately through the magnetic midplane and the edge LIDAR passes tangential to the flux surfaces, giving high resolution observations of the plasma edge. The lines of sight are shown in figure 1a.

Models

For each diagnostic, a 'forward model' is created which predicts the distribution of measurements that could be observed given a predefined physical state. The interferometry is modelled simply by integrating n_e along its lines of sight but the LIDAR model is considerably more complex, depending on many extra calibration/auxiliary parameters. Figure 1 shows the lines of sights of the three diagnostics and an overview and sample output of the LIDAR model.

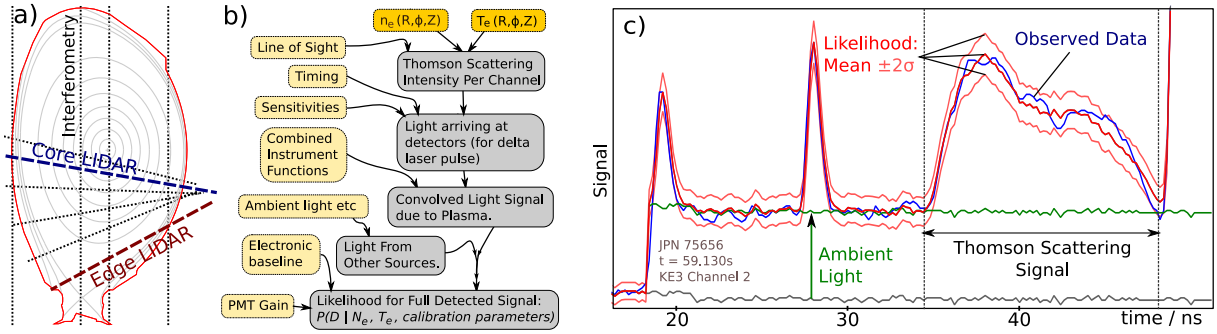

Figure 1: a) Poloidal cross-section of JET and lines of sight of interferometry (dotted), core and edge LIDAR (dashed) and typical flux surface geometry (gray). b) LIDAR Forward model outline using physics parameters (yellow) and calibration/other parameters (light yellow). c) Core LIDAR digitiser trace for spectrometer channel 2 showing observed data (blue) and likelihood distribution mean (red) and $\pm 2\sigma$ (light red) from the model.

In the standard analyses, the auxiliary parameters must be fixed to calibration measurements or determined by statistical cross calibration with other diagnostics. While these can be used as

*See the Appendix of F. Romanelli et al., Fusion Energy Conference 2008 (Proc. 22nd Int. FEC Geneva) IAEA

the prior distribution for the parameters here, there is sufficient information from the combined systems to use weak priors in many cases. In particular, because the spectrometer sensitivities of the edge LIDAR system are difficult to determine (and to demonstrate the applicability of the technique to cases where some calibration parameters are completely unknown), these parameters are assigned effectively no prior information - a uniform distribution. The timing parameters which effect inferred positions, are also assigned uniform priors.

For the plasma, n_e and T_e are assumed constant on any poloidal flux surface so are modelled as 1D functions of poloidal flux ψ_N (normalised to 0 at the magnetic axis and 1 at the last closed flux surface). A linear interpolation of 40 'knots' at fixed positions is used, with more in the H-Mode pedestal region (see figure 2a/b). The knot magnitudes are the parameters for which the posterior is obtained. For this work, the single fixed $\psi_N(R,Z)$ provided by the EFIT code routinely used at JET [4] is used. This makes strong assumptions about the current and pressure profiles and may introduce systematic errors in ψ_N to which the combination of the core and edge LIDAR systems is especially sensitive, due to their distant lines of sight. To correctly deal with this in the Bayesian analysis, ψ_N should be taken from a model based on plasma parameters included in the inversion. Such a model has been previously developed[11] and will be used in future results.

Results - A typical posterior

The posterior distribution gives the probability for any combination of the plasma and calibration parameters and so describes all of the information that can be known about these parameters, given all the prior assumptions and all the observations. It includes both the systematic and random uncertainties from all modelled sources. (For previous examples of the procedure, see e.g. [5, 6]). To examine this high-dimensional distribution, a series of representative samples are drawn. Each sample is a complete description of a possible state of the entire system, that is consistent with all the diagnostics. They can be displayed separately or used to generate histograms for each parameter, giving the marginal distribution which expresses what can be inferred about that parameter, independent of all others. Figure 2 shows several samples (a/b) of the n_e and T_e profiles for a time point in a typical H-Mode JET plasma, as well as the marginal distributions (c/d) for regular points along the N_e and T_e profiles from the same posterior. The time point used lies between ELMs, where the profiles are unlikely to have evolved over the few milliseconds between the capture/integration times of different diagnostics.

Despite the complete freedom (uniform prior distributions) given to many of the calibration parameters which must be fixed in the standard approach, the results are good and many benefits of the integrated approach can be seen. The overall magnitude of the density differs to the standard analysis of core LIDAR due to the inclusion of the Interferometry diagnostic's accurate integral information. The profiles also show much more is inferred in the pedestal region than the core LIDAR standard analysis shows. While this appears entirely due to the edge LIDAR data, core LIDAR provides much of the information. Because the priors given for many of the edge LIDAR calibration parameters were weak in this case, edge LIDAR alone is not sufficient to determine the pedestal profiles. For instance, while the edge LIDAR data can be used to find the n_e pedestal shape, it cannot give its magnitude as the overall sensitivity of the optics is not known and so the prior on that parameter was uniform. The same is true for core LIDAR, meaning it provides the edge pedestal density only relative to the core. The interferometry absolute density information completes the picture and so, without stronger prior information, only together can the three systems provide the profile.

The inference of the T_e pedestal is similarly complex because the priors for the edge LIDAR spectrometer sensitivities were also uniform. The edge LIDAR data alone does heavily constrain the possible sensitivity combinations because the same set must be consistent for the entire

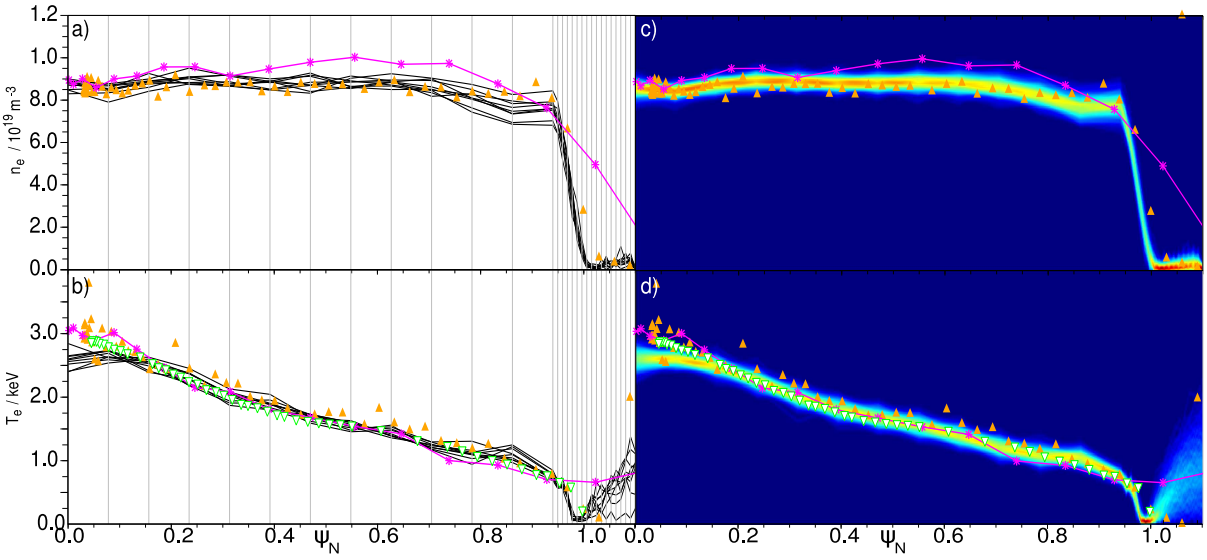

Figure 2: Profiles of electron density (a) and temperature (b) vs normalised poloidal flux of 8 samples from the posterior distribution inferred from core LIDAR, edge LIDAR and interferometry with weak calibration parameter priors. c/d) Marginalised posterior distribution for points along normalised poloidal flux. Also shown are the parametrisation knot positions (vertical lines on a/b) and profiles from routine analysis of the High-Resolution Thomson Scattering[7] (orange △), Electron Cyclotron Emission Heterodyne Radiometer[8] (green ▽) diagnostics and the standard analysis of core LIDAR (magenta * and line).

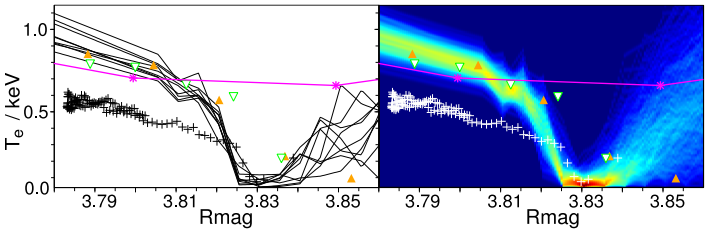

Figure 3: T_e profile samples (left) and marginal distributions (right) on the magnetic axis plane ($Z = Z_{mag}$) vs major radius R_{mag} for the outboard plasma edge. Other diagnostics as in figure 2 with edge LIDAR standard analysis (black/white +) based on spectrometer sensitivity values from calibration.

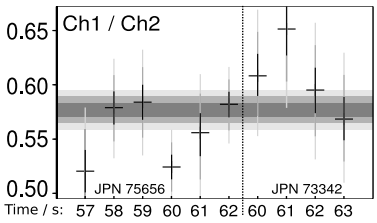

Figure 4: Posterior distributions for sensitivity ratio of two edge LIDAR spectrometers for several time points (2 pulses). Bars show mean and 1σ (black), 2σ (dark gray) and 3σ (light gray). Bands show combined result.

profile but there remains a degree of freedom which is always enough to allow any pedestal T_e. The core LIDAR system, with well determined sensitivities, can in principal provide the edge temperature but lacks the resolution to do this by itself. Consideration of the instrument convolution (which is included in the model but not in the standard analysis) increases the effective resolution but shows that practically, it is a $\sim 12cm$ spatial integral of T_e that is really known. Combined with shape information from the edge LIDAR data, it is just sufficient to reconstruct the profile. Figure 3 shows the inferred T_e profile for just the edge region plotted against major radius. Also shown is the result from the standard analysis of the edge LIDAR data which uses the existent calibration values. An investigation of the discrepancy is underway but the uncertainty in these parameters, while difficult to treat in the standard analysis, is rigorously and inherently handled with the Bayesian approach.

The posterior distribution also describes what can be inferred about the calibration parameters themselves. For a selection of times in 2 pulses, samples of the posterior were obtained and the ratios of the spectrometer sensitivities taken from each (shown in Figure 4). Each one represents what can be known about that parameter from the model, prior and that data. Shown as bands

is the combined distribution which could be used as a prior for future inversions.

Pedestal Parametrisation

It is often useful to use a stronger plasma parametrisation in order to directly obtain the posterior over quantities of interest. For instance, the n_e pedestal is believed to be well approximated by a hyperbolic tangent function[9] of which the width is of particular interest as its scaling with parameters such as ion gyro radius have particular importance for ITER[10]. Figure 5 shows the posterior distribution for the pedestal width w, obtained using the parametrisation $n_e = n_e^{ped}(\,1+\tanh(2(\psi_0-\psi_N)/w)\,)$ added to the knot parametrisation for the core. Samples of $n_e(\psi_N)$ are also shown. The strong assumption of shape, when valid, is particularly useful if the LIDAR signals are weak as in this case where the data has a noise level of $\approx 15\%$, which can be seen to strongly affect the standard analysis.

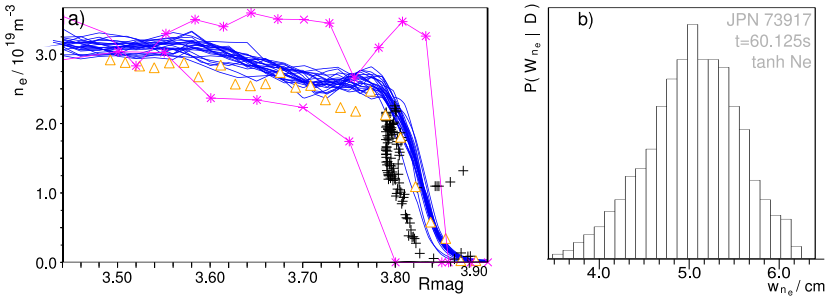

Figure 5: a) Posterior sample profiles (blue lines) determined from tanh parametrisation and others as in figure 3, b) Marginal posterior PDF for pedestal width.

In future work, the posterior will be found for a series of pulses where the quantities of interest (e.g ρ) were varied. From these the information that can be inferred from the LIDAR systems about any relationship of the pedestal quantities on those parameters will be found, supplementing the analysis using the High Resolution Thomson Scattering[10].

Conclusions

The development of a model of the LIDAR Thomson Scattering diagnostic had been outlined and its use to infer electron density and temperature profiles consistent with three systems at JET has been demonstrated. The detail of the model allows the uncertainties and complex relationships of various calibration parameters to be handled easily and rigorously. However, it is necessary to include the model for the plasma current and magnetic diagnostics discussed in section 2 before carrying out the investigation of pedestal parameters described in section 4.

Acknowledgements

This work was partly funded by an EPSRC CASE studentship with UKAEA Culham and has been carried out within the framework of the European Fusion Development Agreement. The views and opinions expressed herein do not necessarily reflect those of the European Commission.

References

[1] G.Braithwaite et al. *Rev. Sci. Instrum*, 60:2825, 1989.

[2] H. Salzmann et al. *Rev. Sci. Instrum.*, 59:1451, 1988.

[3] M. Kempenaars et al. *Rev. Sci. Instrum.*, 79:10E728, 2008.

[4] D.P.O'Brien et al. method. *Nuc. Fus.*, 32:1351, 1992.

[5] R Fischer et al. *Plasma. Phys. Cont. Fusion*, 44, 2002.

[6] J Svensson et al. *4219-4221*, 75, 2004.

[7] R. Pasqualotto et al. *Rev. Sci. Instrum.*, 75(10):3891–3893, 2004.

[8] E. de la Luna et al. *Rev. Sci. Instrum.*, 75:3831–3833, 2004.

[9] R.J. Groebner et al. *Plasma. Phys. Cont. Fusion*, 44:A265–A272, 2002.

[10] M.N.A. Beurskens et al. In *Proc. 36th EPS Conference on Plasma Phys., Sofia, Bulgaria.*, 2009.

[11] J. Svensson and A. Werner. *Plasma Phys. Cont. Fusion*, 50:085002, 2008.